Applied Energy 343 (2023) 121254

Contents lists available at ScienceDirect

Applied Energy

journal homepage: www.elsevier.com/locate/apenergy

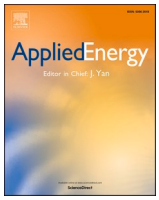

Quantifying the value of probabilistic forecasting for power system operation planning

Qin Wang [a,*], Aidan Tuohy [a], Miguel Ortega-Vazquez [a], Mobolaji Bello [a], Erik Ela [a], Daniel Kirk-Davidoff [a], William B. Hobbs [b], David J. Ault [b], Russ Philbrick [c]

[a] Electric Power Research Institute, Palo Alto, CA 94304, USA
[b] Southern Company, Birmingham, AL 35203, USA
[c] Polaris Systems Optimization, Shoreline, WA 98177, USA

HIGHLIGHTS:

- Development of high-quality probabilistic solar forecasting for present and future solar PV buildouts in Southern Company system.
- A quantitative method is developed to quantify the value of probabilistic solar forecasting for grid operations.
- Transformation of probabilistic forecasts to facilitate grid operations by using a probabilistic dynamic reserve requirement approach.
- Simulation results from the Southern company system show that using dynamic reserves determined from probabilistic forecasts are beneficial to the system compared to using static reserve requirements.

ARTICLE INFO

Keywords:
Probabilistic solar forecasting
Grid integration
Value assessment
Production cost modeling
Dynamic reserves

ABSTRACT

A recent key research area in renewable energy integration is the development of tools and methods to capture and accommodate the uncertainty associated with the forecast errors. While the research community has proposed numerous methods to improve the accuracy of probabilistic forecasts, their application to operational planning is still an open question. This work applies dynamic reserve determination methods to solar probabilistic forecasts and then feed them to a commercial production cost model simulator to assess the value of capturing the uncertainty endogenously in the reserve determination process. Testing is carried out on a calibrated real-size system representing the Southern Company for medium, and high solar penetration levels. Numerical results demonstrate the benefits that can be attained by explicitly modeling probabilistic uncertainty in terms of operating cost, and enhanced system reliability which is measured as the quantity of balancing and reserve violations. Additionally, these methods and results can pave the way for system operators to adopt probabilistic forecasting to draw the operating plans of the system, and this allowing the successful integration of variable renewable energy sources.

1. Introduction

The integration of solar photovoltaics (PV) into electric power grids has been gaining momentum in recent years due to declining costs and technology improvements. As of 2021, the worldwide cumulative installed PV capacity reached about 800 GW, and the total amount is expected to reach 8,500 GW by 2050 [1]. In the U.S., half of the new utility-scale electric generating capacity to be added to the power grids during 2022 will be solar [2]. A recent study from the U.S. Department of Energy shows that solar energy has the potential to supply 40% of the nation's electricity demand by 2035 [3]. With deeper penetrations of solar power in power systems, there is a need for accurate forecasting that includes not only the "*best guess*" but also "*the probabilistic uncertainty surrounding the best guess*". Utilities and independent system operators (ISOs) must manage power grids with increasing levels of stochastic generating resources to maintain reliable and economic operations.

Solar forecasting methods can be divided into two categories: physical methods and statistical methods. The former use numerical weather prediction (NWP) models (usually in medium- and long-term)

* Corresponding author.

https://doi.org/10.1016/j.apenergy.2023.121254
Received 22 August 2022; Received in revised form 14 April 2023; Accepted 2 May 2023
Available online 15 May 2023

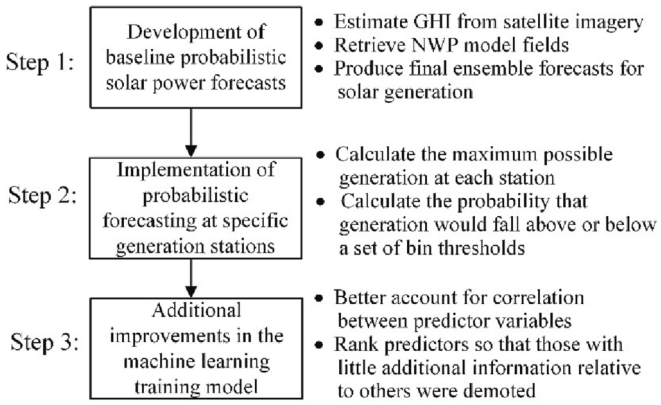

Fig. 1. A summary of the workflow to generate and improve probabilistic solar forecasts.

to forecast solar irradiance, which is then used to calculate the power output from solar PV plants in particular regions. The latter uses historical and/or real-time spatio-temporal data from satellites, sky cameras or from the PV plant itself to correct the results derived from the physical methods or to produce solar power forecasts through statistical models like lag-regression or machine learning. Recent studies have shown that hybrid models of machine learning and numerical modeling may perform better than using them individually [4]. With increasing computer speed and storage capacity, and advancements in machine learning algorithms in the past 15 years, substantial progress has been made in the accuracy of solar forecasting. For instance, the IBM has developed a solar forecasting system that is up to 30% more accurate than the conventional approaches by using machine learning, big data, and analytics to continuously analyze several weather models [5]. However, the output of these physical and statistical models is still a deterministic forecast which provides no information on expected uncertainty.

Many balancing authorities currently use solar forecasting in operations, but they generally rely on single-valued forecasts. Historically, attempts to obtain more value from forecast information have focused on improving the mean-square error (MSE) accuracy with less effort on quantifying the uncertainty of the prediction. This uncertainty is an essential ingredient for optimal decision making in power systems with high renewable penetration levels. A "perfect" deterministic forecast will never be achieved due to the chaotic dynamics of the atmosphere, which increases the risk of balancing the grids in real-time. As such, there is increasing interest in probabilistic forecasts that are tuned to grid events.

Some utilities have taken steps towards the integration of probabilistic forecasts. For example, the Swiss power system operator (Swissgrid) is using probabilistic information to determine balancing reserves required [6]. Hawaiian Electric Light is using an advanced meteorological sensor network to produce high resolution probabilistic forecasts (SWIFT) with greater quantification of uncertainty [7]. California ISO, the Midcontinent ISO, Xcel Energy in Colorado, and others have established ancillary services to manage increasing net-load uncertainty. The requirements for these products, often termed flexible ramping products or load-following reserves, are usually determined based on observed short-term forecast error [8]. However, requirements are updated on a seasonal basis and capture only historical variability and uncertainty. Also, as renewable penetration increases, updates may be needed closer to real-time based on the uncertainty identified by probabilistic forecasts [38].

Research into probabilistic solar power forecasting is broadly divided into three categories: methodological developments, performance benchmarks, and grid integration impacts. In the first category, researchers focus on developing methods to improve the quality of probabilistic solar forecasting: calibration methods based on the Solar Ensemble System [9], forecasts based on variational Bayesian inference [10], a two-stage probabilistic forecasting algorithm based on bivariate conditional solar irradiation distributions [11], and a kernel dressing technique based on Bayesian model averaging post-processing [12]. In the second category, researchers focus on benchmark models to evaluate the performance of probabilistic solar forecasting methods: Ref, [13] compared various popular probabilistic solar forecasting methods using a standardized dataset at Folsom, California; Ref. [14] developed an open-source solar forecasting evaluation framework to support the U.S. Department of Energy's Solar Forecasting II program and the broader solar forecast community; Ref. [15] developed a new climatology reference model to benchmark probabilistic solar forecasts. In the third category, there are as yet few published examples and none have focused on benefits of implementing probabilistic solar forecast in power system operations: Ref. [16] conducted a review on the current use of probabilistic solar forecasting in power systems; Ref. [17] described the procurement of ramping product and regulation in California ISO using probabilistic solar power forecasts; and Ref. [18] explored the use of probabilistic renewable power forecast in stochastic optimization.

Ref. [39] developed a method to incorporate uncertainty of wind power generation forecast into power system operation, dispatch, and unit commitment procedures. It proposed three levels of probabilistic tool integration: passive integration which simply displays the probabilistic information in the control center for system operators' situational awareness, active integration which uses uncertainty information to rerun the unit commitment (UC) and economic dispatch (ED) processes for the worst scenarios, and proactive integration which will add new constraints like the ramping requirement into the UC ad ED models. One weakness of the paper is that it focuses more on high-level descriptions, lacking quantitative analysis. In addition, considering the worst scenario in the "active integration" level may lead to over-conservative operating outcomes. A more practical method to deal with solar uncertainty was proposed in [40], which calculates the reserve requirements of a microgrid by taking into account the solar and load forecasting uncertainty. However, the proposed method has not been tested on bulk power systems. Refs. [42,43] demonstrated that the ISOs can take advantage of probabilistic solar forecast by using it to better determine the reserve requirement of the flexible ramping products, which can lower the generation costs and improve the reliability of power systems. Similarly, Ref. [44] developed a data-driven method to better estimate the system's ramping needs based on short-term probabilistic solar irradiance forecasts. However, these approaches may not apply to the ISOs that have yet introduced the flexible ramping products [8]. Our previous research in [35] has demonstrated a practical approach to determine the dynamic reserve requirements by leveraging probabilistic forecasts, but the approach has not been integrated into the grid operation process. To bridge the gap in the literature, this work develops a quantitative method to quantify the value of probabilistic solar forecasting for grid operations. The major contributions of this paper include: (1) Developed a framework to integrate the probabilistic forecasts into power system operation planning process, (2) Validated the proposed approach using real-world grid operation data from the Southern Company (SoCo) in the U.S. [19,20], and (3) Conducted in-depth analysis on the value of probabilistic forecasts for power system operation planning. Note that although this paper focuses on solar forecasting, the proposed approach also applies to probabilistic forecasting of wind power and system demand.

The reminder of the document is organized as follows. Section 2 presents an overview for the development of probabilistic solar forecasting for various solar PV buildouts. Section 3 proposes a method to transfer the probabilistic information into information that can be consumed for grid operation purposes. Section 4 discusses the production cost modeling (PCM) simulation framework and the design of studied scenarios. Section 5 presents simulation results. Finally, section 6 presents conclusions.

2. Development of probabilistic solar forecasting for present and future solar PV buildouts

2.1. Probabilistic solar forecasting methodology

Ensuring high-quality probabilistic forecasts is key for their successful application. As part of a U.S. Department of Energy funded project "Operational Probabilistic Tools for Solar Uncertainty (OPTSUN)" [24], we have developed new methods that are applied to existing probabilistic solar forecasting practices to produce the improved forecasts. The process is summarized in Fig. 1 and detailed as follows.

1. In the first step, historical and real-time probabilistic and deterministic forecasts of solar generation at real and hypothetical PV facilities of interest are generated by our collaborators at UL. Probabilistic solar power forecast models were developed, and their forecasts were generated for hourly time resolutions up to 168 h ahead, for distributed and central solar PV. These baseline forecasts, delivered for the desired year, were analyzed to assess the potential for forecasting performance improvements. The solar forecast system used in this work includes modules that perform the following functions: (1) Estimating global horizontal irradiance (GHI) from satellite imagery in near-real time; (2) Extrapolating current cloud positions and motion from satellite imagery into the near future, and derive short-term forecasts of GHI from these extrapolated cloud fields; (3) Calculating plane-of-array irradiance given sun position and GHI, including estimation of direct normal irradiance from GHI and sun angle; (4) Retrieving Numerical weather prediction (NWP) model fields from several national weather services, and extract and archive forecasts for fixed locations; (5) Employing a machine-learning system that relates past NWP forecasts to observed generation directly to forecast PV generation from real-time NWP forecasts; (6) Producing final ensemble forecasts of solar generation from forecasts produced by the satellite-based and NWP-based forecast systems.
2. In the second step, probabilistic forecasting was implemented by converting the NWP-based machine-learning system from one that was trained to produce a single-valued forecast for each lead time to one that produced forecasts of the probability that generation would exceed a range of values, fixed fractions of the maximum possible generation at each generation station or aggregate of stations. These forecasts of the probability that generation would fall above or below a set of bin thresholds could then be converted to forecasts of generation at fixed probability-of-exceedance thresholds, by first calculating the cumulative sum of probability over the range of bin edges from zero generation to maximum generation, and then interpolating in the curve to fixed levels of probability.
3. In the third step, additional improvements were developed in the machine-learning training method, to better account for correlations between predictor variables and to rank predictors so that those with little additional information relative to others were demoted. The predictors include NWP model output from the US, UK, German, Canadian, and European weather services, and satellite imagery processed to provide an estimate of surface solar irradiance, as well as recent observations of generation that provide predictive skill due to persistence. Persistence arises in solar generation from the spatial and temporal autocorrelation of surface irradiance, which itself arises largely from the spatial and temporal scale of clouds. These methods resulted in significant improvements in the forecast skill as measured by the Ignorance Score [21], from 5% to 10% compared to the original quantile regression method. More metrics to evaluate the performance of the probabilistic solar forecasting are shown in Appendix A.

2.2. Development of probabilistic solar forecasts for future buildout of power systems

Simulations of operational probabilistic forecasts and actual production were also needed for the expected solar buildout in the future. In this section, we use the SoCo system as an instance to demonstrate how the solar PV generation and probabilistic forecasts of solar PV generation were generated for future buildout. Generation stations were assumed to be of fixed size (25 MW) and were distributed in random clusters, subject to land use constraints with a preferred proximity to population centers, and a minimum separation of 3 km, to represent a preference to constrain excessive aesthetic impacts on communities. The DC/AC ratios were set to be 1.5 in accordance with SoCo's expectations. To generate timeseries of generation, satellite based GHI analysis method was used. We obtained approximately 160,000 visible and infrared satellite images from the GOES 16 satellite [22] on a grid with a horizontal resolution of approximately 0.5 km at 60-minute intervals for 2018 through 2020. These images were analyzed to generate estimates of global horizontal irradiance on the same horizontal grid.

1. The first step in the process of generating accurate GHI estimates from geostationary satellite images involves an explicit calculation of atmospheric transmissivity using the red visible channel imagery. The forward transmissivity calculation involves first the generation of a climatology of minimum pixel brightness at each hour of the day, so that variations in surface reflectivity are removed from the signal of total reflectivity, and correspondence of reflectivity to atmospheric reflectivity are maximized.
2. In the second step of the process, a machine-learning model is trained to use the transmissivity calculated from the red visible channel, along with radiances from multiple infrared channels and the blue visible channel reflectivity, and solar azimuth and zenith angle, as well as satellite view angle to predict surface observations of global horizontal irradiance from sources such as the Surfrad, Solrad, and ARM networks. Once these GHI timeseries were generated, the PVlib python library [23] was used to synthesize the resulting generation timeseries from 25 MW solar farms, some with fixed panels tilted toward the south at an angle two degrees less than the local latitude, some with north–south oriented single-axis solar tracking. According to the preferences of the collaborators at SoCo, a 1:4 ratio of fixed to tracking plants in SoCo's service area was used.

By using the approaches described above, we developed the probabilistic forecasts of solar generation for both present and future solar PV buildouts at three targeted utilities in the U.S., as part of the OPTSUN project. Test results show that our approach has resulted in a 5–10% improvement in forecast skills compared with conventional methods.

3. Transformation of probabilistic forecasts to facilitate grid Operations: A probabilistic dynamic reserve requirement approach

Although the probabilistic forecasts contain more information than the deterministic forecasts, they cannot be directly used without transformation in today's commercial production cost models, PLEXOS [25], PROMOD [26], MAPS [27], PSO [28], nor in SO-dedicated security-constrained unit commitment (SCUC) and security-constrained economic dispatch (SCED) models [29]. There are generally two approaches to address this issue. The first consists in replacing the deterministic scheduling tool by a stochastic one which allows including scenarios generated from the probabilistic forecast [30–32] to determine the schedule and dispatch considering the uncertainty modeled with the scenarios. The second approach requires transforming the probabilistic information into dynamic reserve requirements (DRRs), which are enforced as reserve constraints in the existing deterministic scheduling models [33–35]. This work focuses on the latter approach

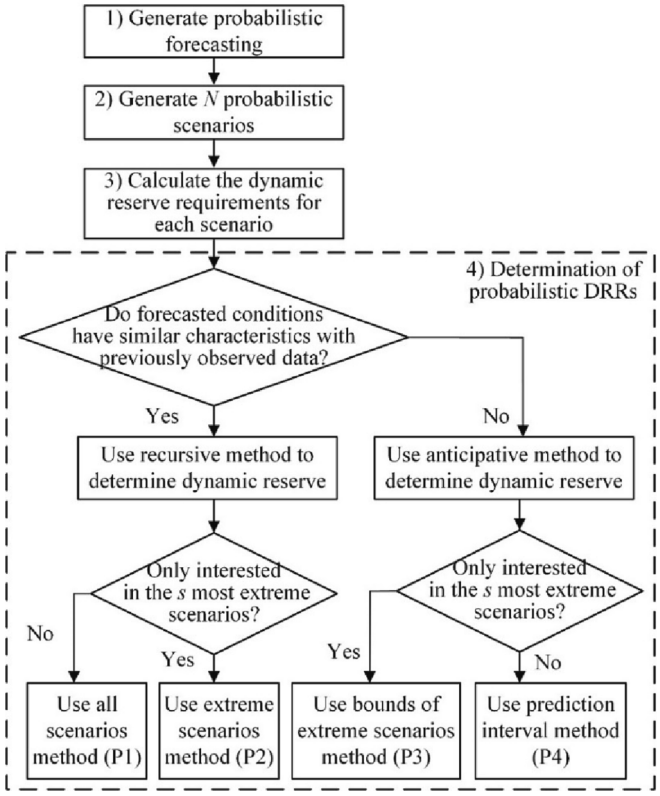

Fig. 2. The process to determine different types of probabilistic dynamic reserve requirements.

since it does not require any modifications to the present scheduling models, nor to the interpretations of results such as energy and ancillary services prices. Detailed formulations of the probabilistic DRR approach are available in our previous publication [35], and it is summarized in Fig. 2.

The method shown in Fig. 2 works as follows: In step (1), the methods described in section 2 are used to generate the probabilistic solar power generation. The step (2) is to transform the probabilistic forecasts into chronologically correlated probabilistic scenarios (see the examples of Figs. 3 and 4 in Section 5). The number of scenarios N is defined by the users and is set to 5000 in this study. The probabilities of the N scenarios can also be calculated with respect to their individual materializations in the various parts of the uncertainty thresholds. In step (3), the system's DRRs are calculated for each individual scenario (i.e., anticipated forecast). Given a desired confidence interval (CI), the DRRs are a quantile function of the exact historical reserve needs which are the difference between actual quantities and forecasted quantities. In step (4), the probabilistic DRRs are calculated. Five different approaches could be used to determine the probabilistic DRRs:

i. All scenarios method (P1), where all the scenarios determined in step 2 will be used. The expected requirements are the weighted sum of the DRRs calculated in step 3 for all scenarios with the weight factors being the probabilities of the scenarios.
ii. Extreme scenarios method (P2), where only extreme scenarios in step 2 will be used. The expected requirements are the weighted sum of the DRRs for extreme scenarios.
iii. Bounds of extreme scenarios method (P3), where historical forecast data is not needed and only the expected worst upward and downward scenarios (i.e., the extreme scenarios) will be used. The probabilistic DRRs are the difference between the central forecast and the weighted sum of the probabilistic forecasts for the extreme scenarios (determined in step 2).
iv. Prediction interval method (P4), which uses the cumulative distribution function (CDF), denoted as $F(\bullet)$, of probabilistic forecasts directly. Given the desired prediction interval α, the probabilistic DRRs are the difference between $F^{-1}(1-\alpha)$ and $F^{-1}(0.5)$ where $F^{-1}(\bullet)$ is the inverse function of the CDF.
v. Hybrid method, which combines any of the four methods above or any other alternatives (e.g., deterministic reserves) available to the user.

According to [35] P1 and P2 are categorized as *recursive* methods, since the DRRs for each of the probabilistic scenarios is obtained from a training done on datasets of historical deviations. The P3 and P4 are categorized as *anticipative* methods, since they rely only on the

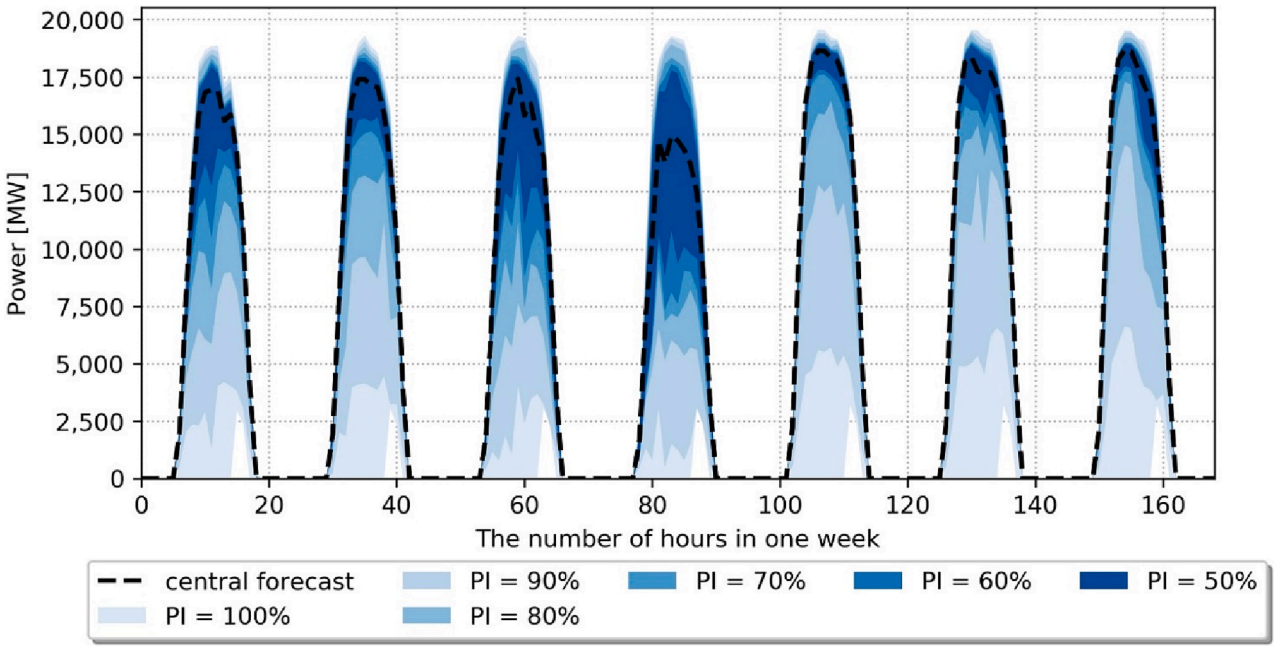

Fig. 3. Probabilistic solar forecasting for one week (Sep. 2nd–8th) in SoCo system with 20 GW solar penetration.

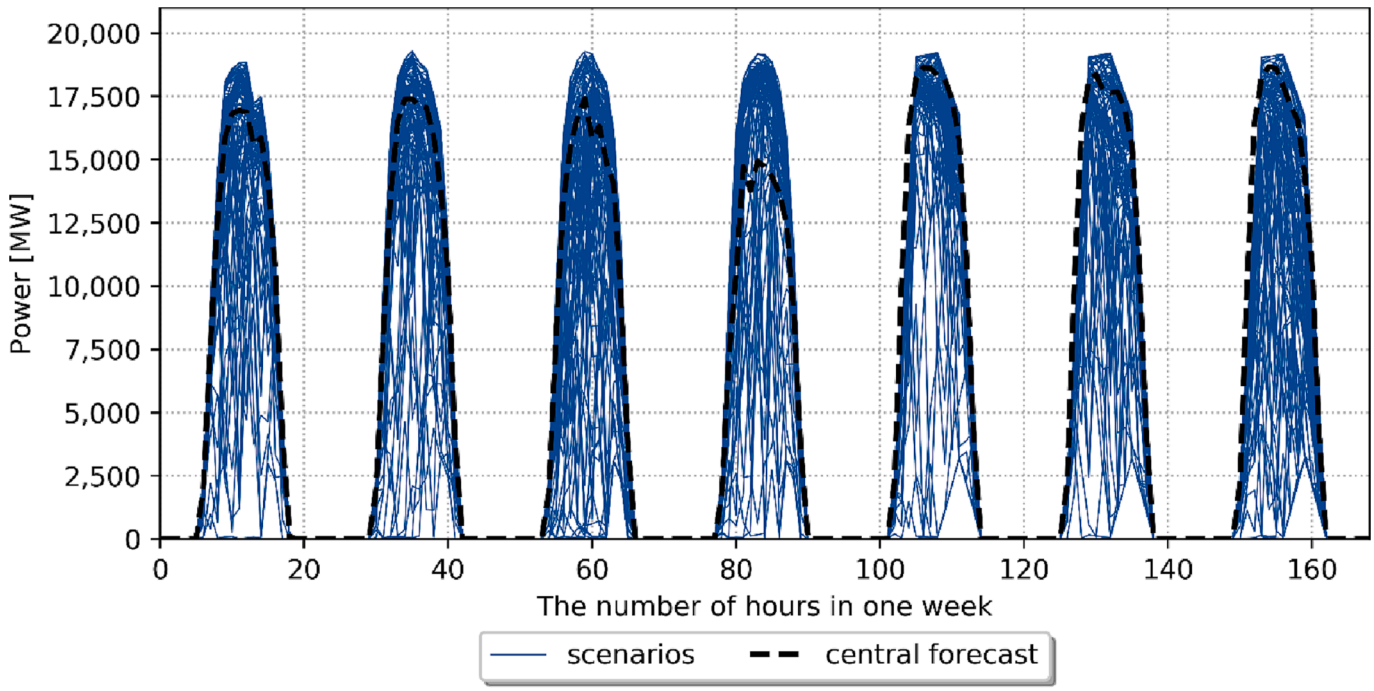

Fig. 4. Probabilistic scenarios generated from the probabilistic solar forecasting for Sep. 2nd–8th in SoCo system with 20 GW solar penetration.

probabilistic forecasts to calculate the DRRs. Hence, the P1 and P2 are suitable for cases when the forecasted conditions have similar characteristics with previously observed data, and P3 and P4 are suitable for capturing the "unique" events that may not be observed in historical data (e.g., weather-driven events). A fifth category is composed by hybrid methods that combine the benefits of recursive and anticipative methods and that has the potential of outperforming any of the induvial recursive or anticipative methods. The formulations of the P1 to P4 methods are shown in Appendix B.

4. Modeling and production simulation for the SoCo system

4.1. Description of the SoCo system for base case study

A calibrated model of the year 2019s SoCo system is used to benchmark the base case modeling, and two future cases with increased levels of solar penetration are examined. The entire SoCo balancing area footprint is modeled in this work. SoCo had a 2019 peak demand of about 38,500 MW which occurred in mid-August. The annual demand was met by coal (22%), natural gas (50%), nuclear (16%), and renewables, including hydro (12%). The total solar generation capacity in 2019 was about 2.3 GW. SoCo has a long-term emissions reduction goal of net-zero emissions by 2050. To meet the goal, solar power generation is expected to play a significant role. The base case has, by nameplate capacity: 15% coal, 59% gas, 5% nuclear, 11% oil, 9 % biomass, and 1% pumped storage (PS). The hydro, wind and solar are modeled on the system-level rather than at the individual resource level. Hourly time-series data for hydro, wind and solar generation and system demand for 2019 were provided by SoCo. The solar forecasting and generation data for future high-solar scenarios were determined with the approach described in section 2. Other operating characteristics and parameters needed for the model include:

i. *Fuel price*: The fuel prices of coal, natural gas and oil at each facility were provided by SoCo on a monthly basis, with the same prices used for all future periods. This may be unrealistic in terms of the absolute numbers for production costs, but as the focus is on comparison of different uses of forecast information, it is not likely to have a significant impact.
ii. *Modeling of pumped storage units*: There are three pumped storage hydro (PSH) units in SoCo. These units can run in both generation and pump modes. When running in pump mode, the maximum limit and minimum limit of the unit are identical, i.e., it can only provide a fixed quantity of load consumption. When running in generation mode, there are two units whose maximum limit and minimum limit are identical (i.e., they cannot provide flexible services) and there is one unit whose minimum limit is smaller than its maximum limit (i.e., it can ramp up and down while being dispatched). In addition, in the simulations, additional constraints are added to the model to prevent simultaneous charging and discharging for all generators and pumps at a reservoir.
iii. *Outages of units*: the outage data for each unit was provided by SoCo on a seasonal basis.
iv. *Operating characteristics of conventional resources*: The operating characteristics of the thermal power plants such as combustion turbines, combined cycle gas turbines, steam resources and nuclear resources were obtained from SoCo, including a resource's minimum generating capacity, maximum generating capacity, ramp-up rate, ramp-down rate, minimum off time, minimum run time, startup time, shut-down time, fixed costs such as startup, shut-down and no-load costs, fuel costs and incremental heat rates. In some cases, these were summarized based on average data for the fleet, to avoid the need to provide detailed confidential information.
v. *Load*: Hourly resolution aggregated load data for the SoCo system for two historical years were provided by SoCo.
vi. *Wind and solar capacity*: Compared with solar, the capacity of wind resources in SoCo is relatively low. The maximum value of the total wind generation in 2019 was less than 300 MW, while the maximum value of solar generation was almost 2 GW in 2019.
vii. *Wind forecast and generation*: The hourly resolution aggregated wind generation data from two historical years were provided by SoCo. The data includes both the day ahead forecast and the actual output in real-time. The forecasted and actual wind output

Table 1
A comparison of static and dynamic upward reserve requirements for SoCo system.

Reserve Method	Reserve Type	Reserve Requirement in 2WA and DA cycles	Reserve Requirement in 2HA cycle
Static Reserve Requirement	Regulation	*r*	*r*
	Contingency	2,000-*r*	1,250-*r*
	Operating	3,000	3,000
Dynamic reserve requirement	Regulation	*r*	*r*
	Contingency	1,250-*r* + Dynamic Reserve	1,250-*r*
	Operating	3,000	3,000

data is used to determine the reserve requirements along with the solar data.

viii. *Regulation up and down reserves*: The regulation up and down reserve requirement in SoCo system varies over time, with an average value of about 500 MW over a year. SoCo provided the hourly resolution time-series data of regulation up and down reserve requirements from one historical year.

4.2. SoCo's scheduling process

In the SoCo model, cycles are used to represent decision making processes. Each cycle is a "rolling horizon" model used to mimic a specific decision process. A "multi-cycle" modeling framework is adopted to simulate the operating decision processes with fidelity. In this study, three operating cycles are modeled for the simulations to reflect the operational processes of SoCo:

- *Two week-ahead* (2WA): The 2WA cycle, which happens once per day, determines the commitment status of units with long minimum on/off time (≥24 h). The fuel types of these units include nuclear, coal and natural gas. The optimization horizon of the 2WA cycle is 14 days from D + 1 to D + 14 where D is the day in which the decision is made. In the SoCo power system, the maximum value of the minimum on/off time of the thermal units is assumed to be 168 h (or 7 days). These include some coal, nuclear and natural gas units. Hence, the optimization horizon of the 2WA cycle is long enough for the system to make effective unit commitment (UC) decisions for those units.
- *Day-ahead* (DA): The DA cycle, occurs once per day, a day in advance of actual operation, and it serves to commits units with start-up time and/or minimum on/off time are greater than 2 h but less than 24 h. The optimization horizon of the DA cycle is 2 days from D + 1 to D + 2 where D + 1 is the day when the final decisions are made and D + 2 is the look-ahead period.
- *Two-hour ahead* (2HA): The 2HA cycle commit units whose start up time and/or minimum on/off time are less than or equal to 2 h. The 2HA UC process will be run for each hour. The optimization horizon of the 2HA cycle is H + 2 to H + 4 where H is the hour in which the decision is made. The purpose of the 2HA cycle is to efficiently plan near-term resource commitments in the real-time market

Note that the SoCo system does not have a typical 5-minute real-time (RT) dispatch cycle, since the RT dispatch is conducted in the Energy Management System with automatic generation control for every 4 s. Also note that SoCo can make additional updates to the plan between the decision times indicated here, and thus have more flexibility in actual operations.

4.3. Assessment of reserve requirements in the SoCo system

The SoCo system uses static contingency and operating reserve requirements for operations together with time varying regulation requirements, as shown in Table 1. Four types of reserves are implemented, including regulation up, regulation down, contingency reserve and operating reserve. The activation time for regulation up/down reserves is 10 min. The contingency reserve is provided by resources that can be brought online in ten minutes, including quick start combustion turbine units. Once a unit is called on to provide the contingency reserve, it must be available for at least 30 min. The operating reserve is provided by units that are capable to respond in 90 min and are able to provide service for at least 90 min. The regulation reserve requirement, denoted by *r*, varies by hour but the same amount is procured by hour for each day. The regulation reserve can substitute for the contingency reserve, and the Contingency reserve can substitute for the Operating reserve. In the 2WA and DA cycles, the total requirement for Contingency reserve and Operating reserve is 2000 MW and 5000 MW respectively. Table 1 also shows the settings for dynamic reserve requirements that were implemented as a focus point in this article.

Instead of adding a new type of reserve called "dynamic reserve" or "flexibility reserve", this study incorporates the dynamic reserve into the contingency reserve, i.e., setting the new contingency reserve requirement to *1250-r + Dynamic Reserve*, where the *Dynamic Reserve* can be obtained with either deterministic forecasting or probabilistic forecasting using the method described in Section 3.[1] As that reserve is released in real time, it is essentially replacing a 750 MW static requirement in the DA time frame (2000 MW minus 750 MW). This allows for the capacity that is released in RT to manage forecast error to vary, while still maintaining the 1250 MW contingency reserve requirement to cover outages. The aim of the study is thus to compare the performance of dynamic reserve requirement to the performance of the 750 MW static requirements. This comparison is then extended to the different methods proposed in [35] to compute the dynamic reserve requirements using probabilistic forecasts.

Since the capacity of wind power is relatively low compared to solar power in the SoCo system, we only investigated the probabilistic forecasts for solar power. However, the impact of wind power on the reserve determination has been considered in the model—by using deterministic wind forecast data. In Eq. (A1) of Appendix B, the exact reserve requirement ε_t is the difference of the forecasted generation and the actual generation for both wind and solar. On the other hand, we think that it is necessary to consider probabilistic wind forecasts when the wind capacity in the system is high. Under this circumstance, *N* probabilistic scenarios will be generated for both wind generation and solar generation in step 2) of Fig. 2.

5. Study results and analyses

In this work the Power System Optimizer (PSO) software tool [36] is used to model the scheduling process of SoCo system. To evaluate the benefits of using probabilistic forecasting for grid operations, the scheduling results using PDRRs are compared to those obtained using DDRRs, where the PDRRs are obtained from probabilistic forecasts and the DDRRs are obtained from deterministic forecasts. The metrics using for the comparisons include total fuel cost, total production cost, reserves violation, and power balance violations, which have been used for similar studies, [20,37].

The base case, which represents the current operating conditions for the SoCo system and contains about 2 GW solar, was implemented at first. Results for the base case model are used to validate the model and compared with the actual operating data in SoCo system. Although satisfactory results were obtained from the base case model, they were not subjected to the level of validation normally applied to operational models; the focus of this project was to show the value of probabilistic

[1] Note that this is valid only when the new reserve has the same activation time as the contingency reserve. In other systems if the activation times are different, a new reserve will need to be defined.

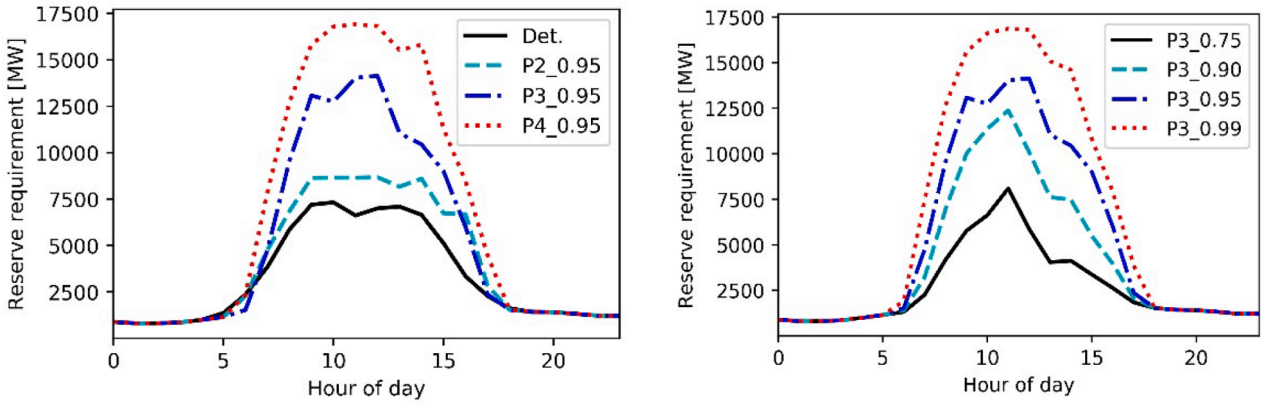

(a) Different dynamic reserve methods

(b) Different confidence intervals

Fig. 5. Dynamic reserve requirements obtained with different methods and confidence intervals on day Sep. 2nd on SoCo system.

Table 2
Annual simulation results on SoCo system with medium solar.

Methods	Det.	Static	P3 (90%)	P3 (99%)	P4 (90%)	P4 (99%)	Hybrid
Annual fuel cost w/o penalties ($)	2,997 M	2,997 M (↑ 0.0%)	2,998 M (↑0.002%)	3,006 M (↑ 0.3%)	2,997 M (↓0.03%)	3,013 M (↑ 0.5%)	3.013 M (↑ 0.5%)
Annual total cost w/ penalties ($)	3,004 M	3,004 M (↑ 0.0%)	2,999 M (↓ 0.17%)	3,008 M (↑ 0.13%)	3,001 M (↓0.09%)	3,013 M (↑ 0.3%)	3,013 M (↑ 0.3%)
Reg. Down violation (MWh)	3,490	3,522 (↑ 1%)	2,831 (↓ 19%)	797 (↓ 77%)	1,934 (↓ 45%)	896 (↓ 74%)	163 (↓ 95%)
Operating reserve violation (MWh)	1,995	2,404 (↑ 20%)	2,323 (↑ 16%)	641 (↓ 68%)	2,048 (↑ 3%)	229 (↓ 89%)	139 (↓ 93%)
Total reserve violation (MWh)	5,485	5,927 (↑ 8%)	5,154 (↓ 6%)	1,438 (↓ 74%)	3,983 (↓ 27%)	1,125 (↓ 79%)	302 (↓ 94%)
Balance violation	0	0	0	0	0	0	0

solar forecasting on higher solar penetration levels of future systems – here, cases with 7 GW solar (i.e., the medium solar case) and 20 GW solar (i.e., the high solar case). Following the guidance from SoCo, modest resource addition and retirement assumptions were made in the 7 GW and 20 GW solar cases.

5.1. Probabilistic solar forecasting results

To facilitate studies for the future scenarios, solar PV generation and probabilistic forecasts of solar PV generation were generated for the SoCo system. Fig. 3 shows the probabilistic solar power forecast for 1 week (Sep. 2nd to 8th) in SoCo system for the future high-solar PV buildout (i.e., 20 GW solar). The dashed back line in the figure shows the central forecast of solar power generation in each hour. The blue areas provide the upper and lower bounds of the solar power generation at different probabilistic thresholds (e.g., 100%, 90%, 80%, 70%, 60% and 50%). For example, the area labeled by "PI (prediction interval) = 90%" means there is a 90% probability that the solar power generation is within the upper and lower bounds of this area. Note that in many hours of the day the lower bounds of 100% PI are relatively low, which leads to wide forecasting areas for the 100% prediction intervals. After conducting a thorough investigation, certain shortcomings were discovered in the lower bounds of the forecast data utilized in this study. Although these shortcomings are unlikely to affect the overall patterns or methodology, they are critical considerations for the application of the research and necessitate further attention in future studies.

5.2. Transformation of probabilistic forecasts

The original probabilistic forecasts in Fig. 3 cannot be used directly in grid operations. Hence, it is necessary to use the method in Section 3 to transform the probabilistic forecasts into chronologically correlated probabilistic scenarios. Fig. 4 shows the probabilistic scenarios generated from the data in Fig. 3. Note that the transformation in Fig. 4 contains the same information as Fig. 3 but in a useable format.

5.3. Dynamic reserve results

Fig. 5 shows the dynamic reserve results on a specific day (i.e., Sep. 2nd) on SoCo system with 20 GW solar. Fig. 5 (a) shows the curves of deterministic dynamic reserve requirements (DDRRs) and three probabilistic dynamic reserve requirements (PDRRs) with 95% CI. The reserves obtained with P1 are not presented since by considering all scenarios, they tend to the average (most likely materialization) which is what is also obtained when using the best guess in the deterministic method. It is observed that on this specific day the P4 method leads to larger DRRs than the P3 method, P3 method higher than P2 method, and P2 method larger than deterministic method. However, this may not always be the case on days with different probabilistic forecast. Fig. 5 (b) shows how the DRRs change with CI values under the same method. Using high CI values lead to larger the reserve requirements since a wider spread of the uncertainty is being covered.

5.4. Annual production simulation results

In this case, multiple methods were used to compute dynamic reserve requirements for a year horizon in SoCo as described in Section 3. Annual production cost simulations are conducted for the reserve requirements obtained with each of the described models. Selected simulation results for 7 GW and 20 GW solar cases are shown in Table 2 and Table 3 respectively. Results from the deterministic (Det.) method are used for benchmarking. The deterministic forecasts were set to 50th

Table 3
Annual simulation results on SoCo system with high solar.

Methods	Det.	Static	P3 (90%)	P3 (99%)	P4 (90%)	P4 (99%)	Hybrid
Annual fuel cost w/o penalties ($)	2,493 M	2,496 M (↑ 0.1%)	2,522 M (↑ 1.1%)	2,631 M (↑ 5.5%)	2,594 M (↑ 4.1%)	2,635 M (↑ 5.7%)	2,632 M (↑ 5.6%)
Annual total cost w/ penalties ($)	2,610 M	2,614 M (↑ 0.16%)	2,635 M (↑ 0.93%)	2,635 M (↑ 0.96%)	2,628 M (↑ 0.67%)	2,639 M (↑ 1.1%)	2,637 M (↑ 1.01%)
Total reserve violation (MWh)	15,406	14,535 (↓ 5.7%)	14,415 (↓ 6.4%)	3,959 (↓ 74.3%)	8,411 (↓ 45.4%)	3,844 (↓ 75%)	3,854 (↓ 75%)
Balance violation (MWh)	19,893	20,383 (↑ 2.5%)	19,269 (↓ 3.1%)	0 (↓ 100%)	4,745 (↓ 76.1%)	0 (↓ 100%)	0 (↓ 100%)

Table 4
Annual average dynamic reserve requirements (MW) under different robustness levels for medium and high solar cases.

Methods	Medium solar (7 GW)				High solar (20 GW)			
	75%	90%	95%	99%	75%	90%	95%	99%
P2	1,660	1,676	1,684	1,693	3,447	3,562	3,617	3,674
P3	1,326	1,431	1,562	1,982	2,258	3,197	3,932	5,066
P4	1,374	1,531	1,764	2,236	2,716	4,262	5,227	5,292

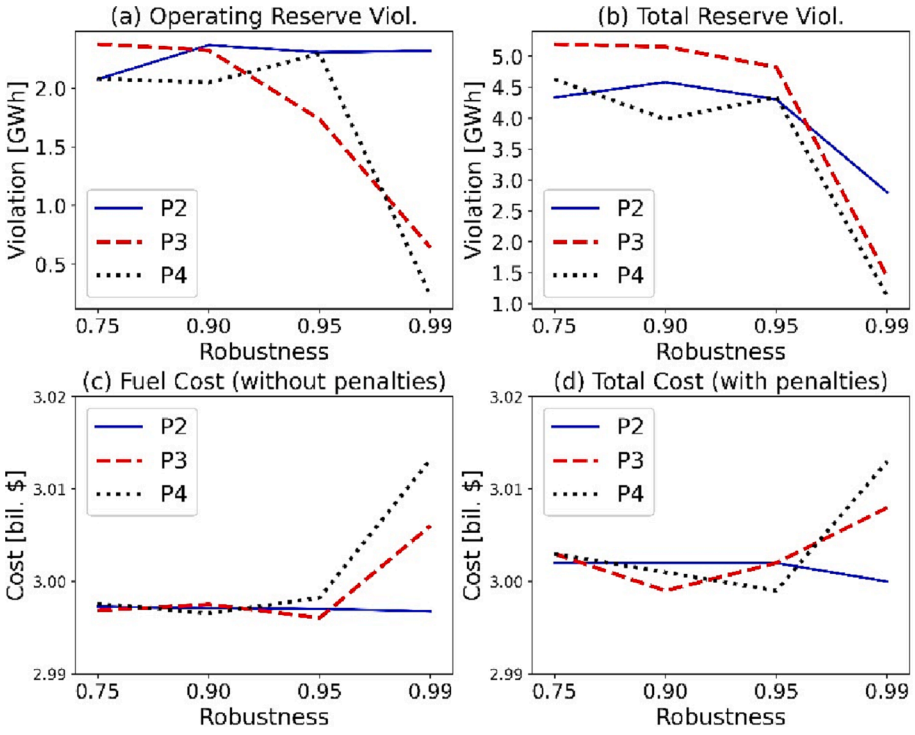

Fig. 6. Sensitivity study results for medium solar case: (a) operating reserve violation in different methods, (b) total reserve violation in different methods, (c) fuel cost of the system in different methods, and (d) total operating cost of the system in different methods.

percentile of the probabilistic forecasts. To make a fair comparison, the static reserve requirement is set to the average value of deterministic dynamic reserves over the whole horizon. Reserve violations and/or balance violations are reported in the tables, and positive values of them mean that there are reserve and/or energy shortages in those cases.

For probabilistic methods, P3 and P4 under 90% and 99% robustness are chosen for demonstration—these are both anticipative methods and therefore only use the probabilistic forecasts, and do not rely on historical data. The results for P1 and P2 methods are presented in the next section. The hybrid method is created by combining P4 (99%) and the deterministic method.

For the 7 GW (medium solar) case, there are no power balance violations in any case, reflecting that the system can successfully accommodate 7 GW solar generation without balancing violations or load shedding. The fuel cost in the table shows the cost from thermal units, while the total cost includes both the fuel cost and the penalties derived from constraint violations. Both are useful results to examine – fuel costs alone are likely more reflective of the actual operating costs and so should be the main result examined, as penalty costs are based on an arbitrarily set penalty value. However, the objective function being optimized for does include the penalty value also, so it is worth understanding how that changes as well. Violations of regulation up and contingency reserve requirements are not found in all the cases. Although regulation down reserve violations are observed in all cases, these are not concern to the system since in actual system operations the system operator should be able to curtail the solar to meet the regulation down requirements (whereas in the study solar is not allowed to be curtailed to provide regulation down reserve), assuming the policy

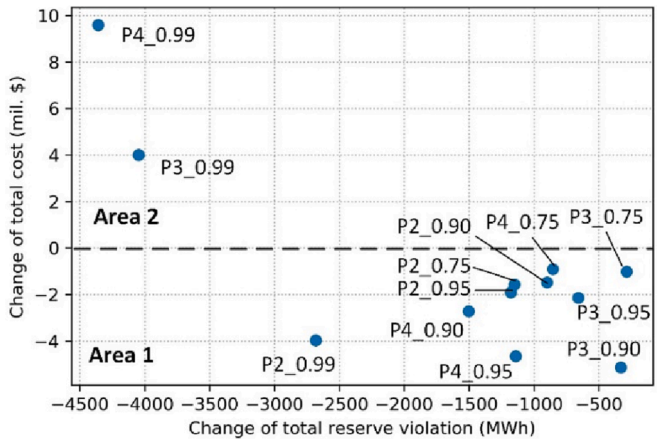

Fig. 7. Scatter plot between change of total reserve violation and the change of total cost for medium solar case.

allows this. It is still useful to examine, but not as important as the upwards reserve violations.

For the operating reserve violations it can be seen that in the deterministic case, of the many hours with violations, there are 4 h where the operation reserve shortage is greater than 300 MW, including hour 18 on Aug. 22th, hour 18 on Sep. 7th, hour 18 on Sep. 8th and hour 11 on Nov. 6th. As shown in Table 2, the reserve violations are reduced significantly by using probabilistic methods. Compared to the deterministic method, the P3 and P4 methods with 99% robustness attain a reduction of 74% and 94% respectively of the total reserve violations, with a modest increase in the total operating cost (increasing 0.13% and 0.3% respectively). The static reserve method results in similar total cost as the deterministic method, but 8% higher reserve violations. The hybrid method is 0.3% more expensive and reduces the reserve violations by 94% compared to the deterministic method, showing that it can attain a good tradeoff between the cost and the reduction of violations. Depending on the risk preference of the operators, and the costs of making updates closer to real time, the hybrid method may be preferred, or a method that improves reliability even further.

In the 20 GW solar (high solar) case, a total of 19,893 MWh of load balance violation obtained when using the deterministic method to set the reserve requirements. The static method results in slightly higher quantity of power balance violations compared to the deterministic method, but the P3 and P4 methods result in significantly lower quantity of power balance violations than the deterministic method. In addition, the quantity of balance violation goes to zero in P3 and P4 with a 99% robustness, at a cost of $140 million. The annual total cost (including the penalty cost of violations) of the P3 (99%) and P4 (99%) is 0.96% and 1.1% higher than the deterministic method respectively.

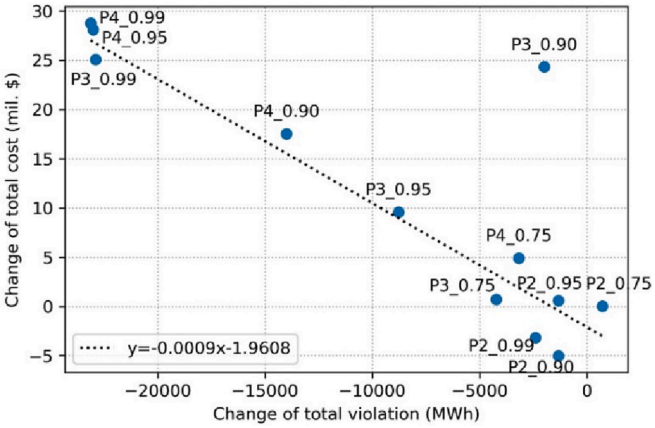

Fig. 9. Scatter plot between change of total reserve violation and the change of total cost for high solar case.

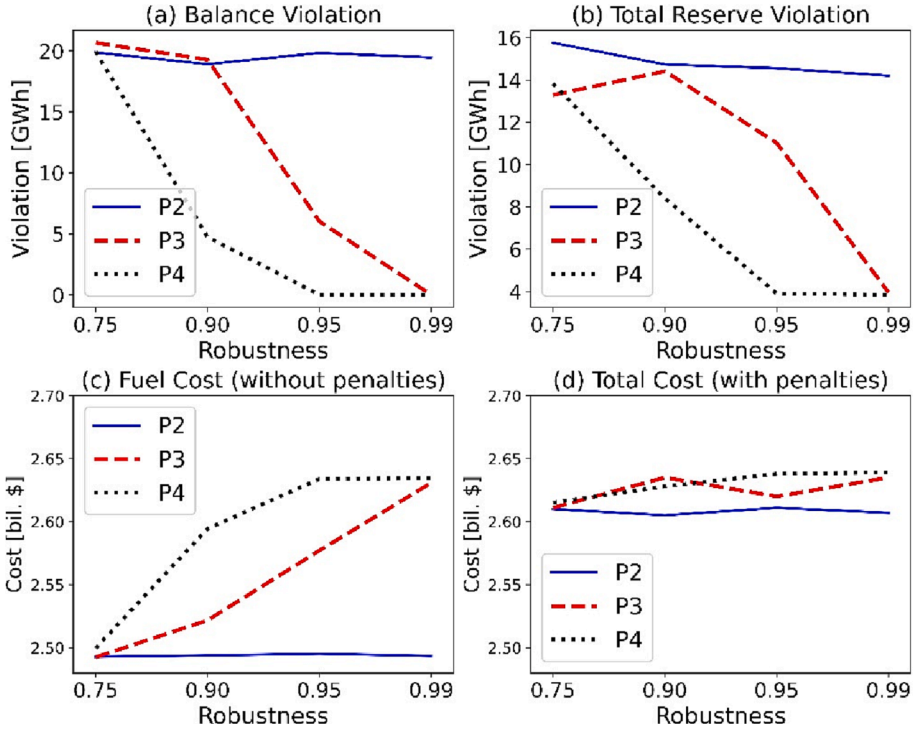

Fig. 8. Sensitivity study results for high solar case: (a) balance violation in different methods, (b) total reserve violation in different methods, (c) fuel cost of the system in different methods, and (d) total operating cost of the system in different methods.

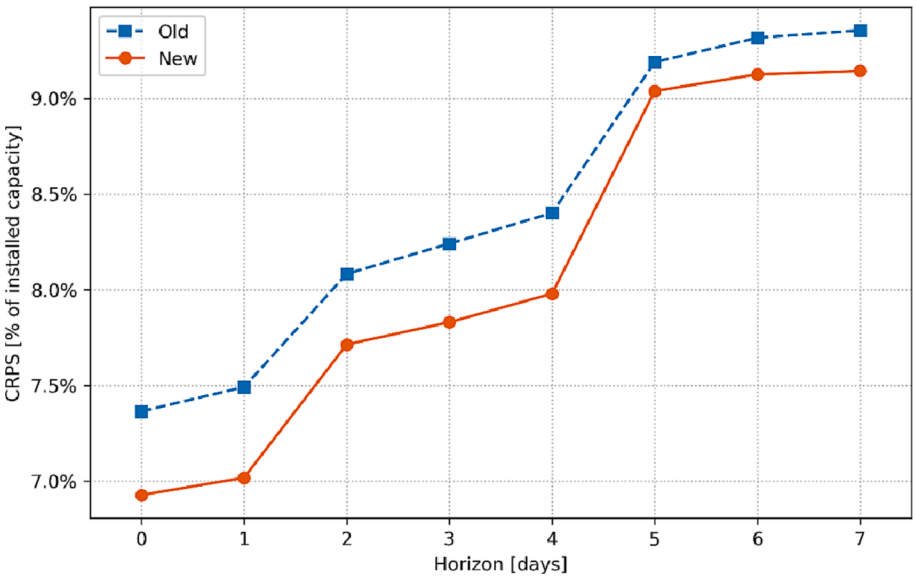

Fig. A1. Improved forecast accuracy (decreased forecast error) between two iterations of the forecast methods (old v.s. new) as measured by the CRPS as a function of the forecast horizon.

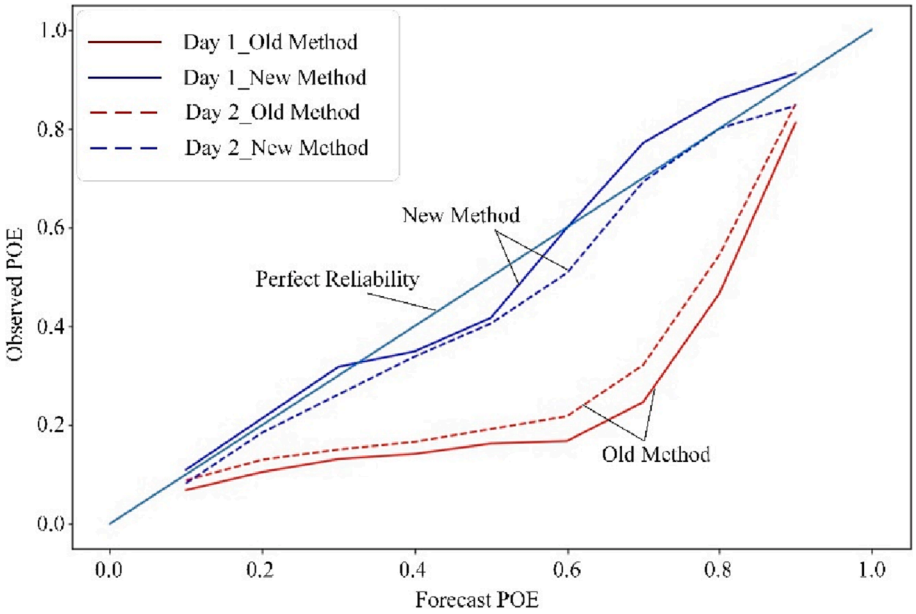

Fig. A2. Forecast reliability between the old v.s. new methods, where the diagonal solid line indicates perfect reliability.

5.5. Sensitivity studies on probabilistic reserve methods

System operators can select different robustness levels for methods P2, P3 and P4, based on their risk tolerance. A challenge for operators is how to select the proper probabilistic method and their corresponding robustness levels for their grid operations. Conducting sensitivity studies sheds light on this challenge. Table 4 shows the annual average dynamic reserve requirements under different robustness levels for 7GW and 20 GW solar cases. Several observations can be made from these two tables: (1) The dynamic reserve requirements in the 20 GW solar case are higher than those in the 7 GW solar case, as expected due to high uncertainty with more solar power; (2) In P2 method, the average reserve requirements slightly increase with the increase of robustness. The difference of the values is relatively small, mainly due to the way the extreme scenarios are used with the recursive method described earlier – picking more extreme scenarios with very high or very low production may result in lower reserves as this scenario may actually be easier to forecast for than those that are less extreme and therefore may exhibit more variability; (3) In P3 and P4 methods, the average reserve requirements increase significantly with the increase of robustness, as would be expected for these anticipative methods where higher robustness results in higher levels of uncertainty being captured; (4) The P4 method sees higher average reserve requirements than the P3 method under each robustness level, which may not be generically true but has been observed in this project.

Fig. 6 shows the sensitivity study results for the 7 GW solar cases with different probabilistic methods and robustness levels. Fig. 6(a) shows the violations of operating reserves in one year in all cases. The operating reserve violation decreases significantly for P3 and P4 methods when the robustness is close to 0.99. Fig. 6(b) shows the total violations of reserves (i.e., sum of operating and regulation reserves) in all cases. For the P3 and P4 methods, the total reserve violations drop slowly

when the robustness level is lower than or equal to 0.95, and then quickly from 0.95 to 0.99. For the P2 method, the total reserve violation slightly increases when the robustness changes from 0.75 to 0.9 (due to the increase in regulation down reserve violations) and then drops when the robustness changes from 0.9 to 0.99. Fig. 6(c) shows the annual fuel costs in all cases. The fuel costs are very close for all the robustness levels in P2 method. In P3 and P4 methods, the fuel costs are similar when then robustness is lower than or equal to 0.95 but increase significantly when the robustness changes from 0.95 to 0.99 (although the absolute value of the change is large, the percentage value is only about 0.3–0.5%). Fig. 6 (d) shows the annual total cost (fuel cost plus penalties for violations) in all cases. For P2 method, the curve decreases slowly, similar to reserve violations; for P3 and P4 methods, the curves decrease first and then increases. Some observations can be made from these results: (1) for the P2 method, it is recommended to use a high robustness value (e.g., 0.99), which leads to lower violations and costs than other robustness values (e.g., 0.75, 0.9 and 0.95); (2) the performances of P3 and P4 methods are similar, thus the operator can select either one in the operations; (3) for P3 and P4 methods, it is recommended to choose 0.90 and 0.95 robustness in normal situations (e.g., demand is not high and renewables output is normal) and 0.99 robustness in higher stress situations (e.g., close to peak demand and/or low renewable output).

To further illustrate the value of using probabilistic forecast, a X-Y scatter plot for the changes of costs versus the changes of reserve violations is used, where the changes are the difference between the probabilistic case and the deterministic case, as shown in Fig. 7. For example, the point P4_0.99 refers to the Prediction Interval (P4) method with 0.99 robustness, and its coordinate (x = −4360 MWh, y= $ 9.6 mil.) means that the total reserve violation is 4,360 MWh lower than the deterministic (D) case and the total cost is $ 9.6 million higher. The vertical axis is the change of annual total cost. The dots in the figure are divided into two areas based on their locations on the plane: (1) dots in Area 1 see lower total cost and lower reserve violations; (2) dots in Area 2 see higher cost and significantly lower reserve violations. This means that if one wants to get a significant reduction in violations, the P3_0.99 or P4_0.99 methods are observed to be more useful; for lower reductions, other methods are more useful given they do not cost as much. As such, one may want to use the more robust levels during periods of higher system stress, e.g., when supply–demand balance is expected to be tight or when large variability is predicted. In addition, if other lower robustness values are used (e.g., ≤ 0.5), the corresponding dots may fall into the area where both higher cost and higher violations are seen. Hence, they are not recommended to use.

Another interesting metric to be evaluated is the per unit cost/benefit of reducing the reserve violations. The coordinate of dot P4_0.99 in Fig. 7 is (−4360, 9.6), which means that $9.6 million cost increase is seen for a reduction of 4,360 MWh of reserve violations in P4 with 0.99 robustness. Hence, the per unit cost is $2,199 for a reduction of 1 MW reserve violation. Similarly, the coordinate of dot P3_0.99 is (−4046, 4), so the per unit cost is $987 for the reduction of 1 MW reserve violation.

The same type of analysis is performed for the high solar case. Different from the medium solar case, it is observed a significant number of power balance violations in the high solar base case. This indicates that the operating conditions of the high solar case could stress the system more heavily. Fig. 8 shows the sensitivity study results of the high solar cases. Fig. 8(a) shows the annual balance violations for each method under different robustness levels. The P2 method only has a marginal impact on the power balance violations (hence the curve is relatively “flat”) as the robustness level varies. The reason is that when the robustness increases, the average reserve requirement in P2 is similar (see Table 4). However, to reduce the balance violation in RT, more reserves should be held in DA, which cannot be achieved by using P2, it is therefore observed that P3 and P4 perform better for the high solar case. For P3 and P4 methods, the power balance violations decrease as the robustness levels increase. Note that there are no power balance violations for P3_0.99, P4_0.95 and P4_0.99. Fig. 8(b) shows the results of total reserve violations. With the increase of the robustness level, the values on the P2 curve decreases, but the values on P3 and P4 curves drop relatively fast. Fig. 8(c) and (d) shows the results of the change of fuel cost and total cost respectively. Again, the curves for P2 methods are relatively flat, but the curves for P3 and P4 methods increase with the increase of the robustness level. The below observations can be made from the analyses: (1) the P2 method only slightly reduces the violations; (2) the P3 and P4 methods can help reduce both the balance violations and reserve violations, but this comes with higher costs. Thus, it is necessary to make a tradeoff between the reduction of the violations and the increase of costs.

Fig. 9 shows the X-Y scatter plots for the changes of total cost (fuel cost plus penalties) versus the changes of total violation (balance violation plus reserve violation) in the high solar case. There is an outlier in the figure, i.e., the dot for P3 method with 0.9 robustness (P3_0.90) where the total violation only has a small decrease, but the overall cost increases significantly. Hence, the P3 method with 90% robustness is not recommended to use for the high solar (20 GW) case. By eliminating this point, the other points in the figure line up very well on the curve $y = -0.0009 \times -1.9608$, which is obtained by a linear regression analysis. The slope of the curve is −0.0009, which means that in order to reduce 1 MWh of total violations, the cost will increase $ 900 (or 0.0009 M$) on average. This curve will help the system operators to make tradeoffs between the reduction on the violations and the increase on the costs while selecting the probabilistic methods.

6. Conclusions

This work proposes a practical approach as well as the modeling framework to quantify the value of probabilistic solar forecasting for grid operations by transforming the probabilistic information into dynamic reserve requirements. Simulation results from the Southern company system show that using dynamic reserves (both deterministic and probabilistic methods) are beneficial to the system (in terms of cost and reduced number of power balance and reserve violations) compared to using static reserve requirements. In addition, the values brought by probabilistic methods are higher than that brought by deterministic methods, indicated by lower balance and reserve violations, at lower or similar operating costs. In general, the benefits brought by the adoption of dynamic reserves are significant (especially in terms of power balance violations reduction) in the high solar penetration case. To best utilize the power of probabilistic solar forecast, system operators need to select a proper probabilistic dynamic reserve determination method and the associated robustness level. The best strategies identified in this article are different in the medium and high solar cases. In the medium solar cases, the performances of the anticipative methods (bounds of extreme scenarios and prediction interval) are similar, thus the system operator could select either one in the operation. Moderate robustness (e.g., 0.9 and 0.95) typically performs well, but in more extreme situations (high demand, high solar variability expected), high robustness (e.g., 0.99) may provide more values. In the high solar cases, the recursive method only slightly reduces the violations, and the anticipative methods appear to help reduce both the balance violations and reserve violations, at higher costs. Thus, the system operator would need to make a tradeoff between the reduction of the violations and the increase of costs associated with increasing robustness.

Future work may include a comparison of the proposed dynamic reserve approach with the stochastic unit commitment approach for benchmarking the benefits of using probabilistic solar forecasting. Additional future work will examine the value of probabilistic solar power ramp forecasting for grid operations.

CRediT authorship contribution statement

Qin Wang: Writing – original draft. **Aidan Tuohy:** Conceptualization, Methodology, Writing – review & editing. **Miguel Ortega-**

Vazquez: Methodology, Writing – review & editing. **Mobolaji Bello:** Project administration, Writing – review & editing. **Erik Ela:** Conceptualization, Methodology. **Daniel Kirk-Davidoff:** Methodology, Writing – review & editing. **William B. Hobbs:** Resources. **David J. Ault:** Resources. **Russ Philbrick:** Software, Writing – review & editing.

Declaration of Competing Interest

The authors declare that they have no known competing financial interests or personal relationships that could have appeared to influence the work reported in this paper.

Data availability

The data that has been used is confidential.

Acknowledgements

The authors thank the U.S. Department of Energy's Office of Energy Efficiency and Renewable Energy (EERE), which supported this work under the Solar Energy Technologies Office Award Number DE-EE0008601 with Electric Power Research Institute.

Appendix A:. Performance of the probabilistic solar forecasting improvement

We developed a gradient-boosted decision tree methods to improve the resolution and reliability of probabilistic solar forecasts. This involved using the decision tree algorithm to determine the probability of generation exceeding a series of fixed fractions of maximum generation, resulting in a set of decreasing probabilities. Taking the resulting vectors of probabilities and generation values, we interpolated in probability of exceedance (POE) to find the generation values corresponding to fixed POE. This methodology (i.e., the new method) resulted in improved reliability of probabilistic forecasts compared with our previous technique, which involved quantile regression based on a history of determinist forecasts (i.e., the old method). A common metric for assessing probabilistic forecast accuracy is the continuous ranked probability score (CRPS) [41]. CRPS compares the probability distribution of the forecast (as a cumulative distribution function - CDF) against the observation, where lower CRPS values indicate more accurate forecasts and a CRPS of zero indicates a perfect forecast. Fig. A.1 shows the decrease in CRPS (increased accuracy) from the improved methods as a function of forecast horizon, with the largest differences in the shorter horizons (~4 days ahead or less).

While CRPS are singular values to quantify forecast performance, it can also be helpful to analyze forecast reliability, a.k.a, calibration. Reliability diagrams provided a visual method to validate forecast accuracy at different probabilities. For example, it can justify if the forecast predicts events that occur 70% of the time with 70% probability. Fig. A.2 compares the reliability of two iterations of the old and new methods, showing that the new method has higher reliability (better agreement with the perfect reliability line shown by the dashed solid line). This is the ideal case, i.e., improved probabilistic forecasts should have both low overall error (as measured by, e.g., Ignorance Score or CRPS) and be well calibrated.

Appendix B:. Dynamic reserve determination based on probabilistic forecasts

There are different ways to determine dynamic reserve requirements based on probabilistic forecasting. If historical data is available, statistical analysis can be conducted on it. For example, one can calculate the exact reserve requirements, which are defined as the differences between actual and forecasted quantities, on days with similar operating conditions, as shown in the following equation:

$$\varepsilon_t = P_t^F - P_t^A, \{t = 1, 2, \cdots, \mathrm{T}\} \in G \tag{A1}$$

where G is the group of data sets (e.g., in days with similar weather conditions), T is the number of historical samples in group G, P_t^A is actual generation at t, P_t^F is forecasted generation at t, ε_t is the exact reserve requirement at t. If $\varepsilon_t \geq 0$, upward reserve will be needed. If $\varepsilon_t \leq 0$, downward reserve will be needed.

Then, the range between the maximum and minimum values of the forecast P_t^F is equally divided into B bins with values at the beginning of each bin to be:

$$v_b = P^{F,min} + \frac{b\left(P^{F,max} - P^{F,min}\right)}{B}, \forall b = 1, 2, \cdots, B \tag{A2}$$

Note that the value of B should be chosen properly to avoid under-fitting (B is too small) and over-fitting (B is too large). All the t samples of ε_t are firstly classified into two categories: upward reserve requirements ε_t^{up} if $\varepsilon_t \geq 0$, and downward reserve requirements ε_t^{dn} if $\varepsilon_t < 0$. Then, each ε_t^{up} and ε_t^{dn} is allocated into the bins, i.e., it falls into the bth bin if $v_{b-1} \leq P_t^F \leq v_b$. In each bin, the samples are ordered from the smallest value to the largest value. If there are n samples in the bth bin, quantile analysis can be conducted based on the desired confidence interval $q \in [0,1]$. When all these are done, the upward and downward reserve requirements for a given forecast x_t under desired confidence interval q can be determined with the following equation:

$$r_t^{up/dn}\big|_{x_t} = q - \text{quantiles of the samples in the } b\text{th bin, if } v_{b-1} \leq x_t \leq v_b. \tag{A3}$$

where r_t^{up} and r_t^{dn} is the upward and downward reserve requirement at time t respectively.

Note that Eq. (A3) is based on deterministic forecast x_t. In order to utilize probabilistic forecast, one needs to transfer it into probabilistic scenarios, as shown in Fig. 4. For each scenarios s, the reserve requirement $r_{t,s}^{up}$ and $r_{t,s}^{dn}$ at time t can be calculated with Eq. (A3). Then, the expected reserve requirements are the weighted sum of $r_{t,s}^{up}$ and $r_{t,s}^{dn}$ for all the scenarios:

$$r_t^{up} = \sum_{s \in S} (\omega_s \bullet r_{t,s}^{up}), t = 1, 2, \cdots, \mathrm{T} \tag{A4}$$

$$r_t^{dn} = \sum_{s \in S} (\omega_s \bullet r_{t,s}^{dn}), t = 1, 2, \cdots, \mathrm{T} \tag{A5}$$

where S is the total number of scenarios, and ω_s is the probability of scenario s. **Eqs. (A4) and (A5) are the formulations to calculate dynamic reserves with the "all scenarios method (P1)".**

Sometimes the system operators may want to obtain the reserve requirements based on the extreme scenarios, rather than the full set of all scenarios. Assume S^{up} and S^{dn} to be the worst upward and downward subsets of scenarios. The corresponding reserve requirements can be calculated with (A4) and (A5) by replacing the full set S with S^{up} and S^{dn} respectively. **This will derive the dynamic reserves with the "extreme scenarios method (P2)".**

On the other hand, the reserve requirements can be obtained purely from the probabilistic forecasts, without using the historical data information. The corresponding methods are called anticipative methods. The expected worst upward and downward forecasts in S^{up} and S^{dn} are shown in the following equations:

$$P_t^{F,up} = \frac{1}{\sum_{s\in S^{up}}(w_s)} \sum_{s\in S^{up}} (\omega_s \bullet P_{t,s}^F), \quad t = 1, 2, \cdots, \mathrm{T} \tag{A6}$$

$$P_t^{F,dn} = \frac{1}{\sum_{s\in S^{dn}}(w_s)} \sum_{s\in S^{dn}} (\omega_s \bullet P_{t,s}^F), \quad t = 1, 2, \cdots, \mathrm{T} \tag{A7}$$

where $P_t^{F,up}$ and $P_t^{F,dn}$ is expected worst upward and downward forecasts in S^{up} and S^{dn} respectively; $P_{t,s}^F$ is the forecast at t in scenario s. Then, the upward and downward reserve requirements can be calculated as the difference between the expected worst upward and downward forecasts with respect to the central forecast:

$$r_t^{up} = P_t^{F,cf} - P_t^{F,dn}, \quad t = 1, 2, \cdots, \mathrm{T} \tag{A8}$$

$$r_t^{dn} = P_t^{F,up} - P_t^{F,cf}, \quad t = 1, 2, \cdots, \mathrm{T} \tag{A9}$$

where $P_t^{F,cf}$ is the central forecast at time t. **Eqs. (A8) and (A9) are the formulations to calculate dynamic reserves with the "bounds of extreme scenarios method (P3)".**

Another anticipative method is to calculate the reserve requirements based on the CDF ($F(\bullet)$) of the forecasts. For a desired prediction interval α (e.g., $\alpha = 0.9$), the upward and downward reserve requirements are calculated in the following equations:

$$r_t^{up} = F^{-1}(0.5) - F^{-1}(\widetilde{\alpha}), \quad t = 1, 2, \cdots, \mathrm{T} \tag{A10}$$

$$r_t^{dn} = -\left[F^{-1}(1-\widetilde{\alpha}) - F^{-1}(0.5)\right], \ t = 1, 2, \cdots, \mathrm{T} \tag{A11}$$

where $\widetilde{\alpha} = (1-\alpha)/2$ and $F^{-1}(\bullet)$ is the inverse CDF. **Eqs. (A10) and (A11) are the formulations to calculate dynamic reserves with the "prediction interval method (P4)".**

References

[1] International Renewable Energy Agency (IRENA), Global energy transformation: a roadmap to 2050; 2019.
[2] U.S. Energy Information Administration. Preliminary Monthly Electric Generator Inventory; April 26, 2022.
[3] U.S. Department of Energy. Solar futures study; September 2021.
[4] Arcomano T, Szunyogh I, Ott E, Hunt B, Wikner A. Hybrid weather prediction: a blend of machine learning and numerical modeling. American Geophysical Union Fall Meeting (virtual). 2020.
[5] Lu S, et al. Machine learning based multi-physical-model blending for enhancing renewable energy forecast - improvement via situation dependent error correction. In: 2015 European Control Conference (ECC); 2015. p. 283–90.
[6] Abbaspourtorbati F, et al. The swiss reserve market: stochastic programming in practice. IEEE Trans Power Syst 2016;31(2):1188–94.
[7] Zack J, Nakafuji D, Brightbill A. Design and evaluation of the distributed solar power production forecast component of the solar and wind integrated forecast tool (SWIFT). In: Proceedings of the 5th international workshop on the integration of solar power into power systems, Brussels, Belgium; 2015.
[8] Wang Q, Hodge B. Enhancing power system operational flexibility with flexible ramping products: a review. IEEE Trans Ind Inf 2017;13(4):1652–64.
[9] Kim JH, et al. The WRF-solar ensemble prediction system to provide solar irradiance probabilistic forecasts. IEEE J Photovolt 2022;12(1):141–4.
[10] Zhang X, Fang F, Wang J. Probabilistic solar irradiation forecasting based on variational bayesian inference with secure federated learning. IEEE Trans Ind Inf 2021;17(11):7849–59.
[11] Kim H, Lee D. Probabilistic solar power forecasting based on bivariate conditional solar irradiation distributions. IEEE Trans Sust Energy 2021;12(4):2031–41.
[12] Doubleday K, Jascourt S, Kleiber W, Hodge BM. Probabilistic solar power forecasting using bayesian model averaging. IEEE Trans Sust Energy 2021;12(1):325–37.
[13] Yang D, Meer D, Munkhammar J. Probabilistic solar forecasting benchmarks on a standardized dataset at Folsom, California. Sol Energy 2020;206:628–39.
[14] Hansen CW, et al. The solar forecast arbiter: an open source evaluation framework for solar forecasting. In: 2019 IEEE 46th photovoltaic specialists conference (PVSC); 2019. p. 2452–7.
[15] Gal La Salle JL, David M, Lauret P. A new climatology reference model to benchmark probabilistic solar forecasts. Sol Energy 2021;223:398–414.
[16] Li B, Zhang J. A review on the integration of probabilistic solar forecasting in power systems. Sol Energy 2020;210:68–86.
[17] Hobbs BF, et al. Pro2R: procurement of ramping product and regulation in CAISO using probabilistic solar power forecasts. SETO Workshop on Solar Forecasting, May 5–6; 2021.
[18] Groß A, Lenders A, Zech T, Wittwer C, Diehl M. Using probabilistic forecasts in stochastic optimization. In: 2020 international conference on probabilistic methods applied to power systems (PMAPS), Liege, Belgium; 2020.
[19] Southern Company. Implementation and action toward net zero; Sep. 2020. [Online]. <https://www.southerncompany.com/content/dam/southern-company/pdf/public/Net-zero-report.pdf>.
[20] Wang Q, Hobbs WB, Tuohy A, Bello M, Ault DJ. Evaluating potential benefits of flexible solar power generation in the southern company system. IEEE J Photovolt 2022;12(1):152–60.
[21] Roulston MS, Smith LA. Evaluating probabilistic forecasts using information theory. Am Meteorol Soc 2002;130(6):1653–60.
[22] GOES Image Viewer. [Online]. <https://www.star.nesdis.noaa.gov/goes/index.php>.
[23] PVLib. [Online]. <https://pvlib-python.readthedocs.io/en/stable/>.
[24] OPTSUN project overview. [Online]. <https://www.epri.com/optsun/project-overview>.
[25] Energy Exemplar. PLEXOS Market Simulation Software. [Online]. <https://energyexemplar.com/solutions/plexos/>.
[26] Hitachi ABB. "PROMOD." [Online]. <https://www.hitachiabb-powergrids.com/offering/product-and-system/energy-planning-trading/market-analysis/promod>.
[27] General Electric Company, "MAPS." <https://www.geenergyconsulting.com/practice-area/software-products/maps>.
[28] Polaris Systems Optimization. Power system optimizer (PSO). [Online]. <http://psopt.com/pso/>.
[29] Wang Q, McCalley JD, Zheng T, Litvinov E. A computational strategy to solve preventive risk-based security-constrained OPF. IEEE Trans Power Syst 2013;28(2):1666–75.
[30] Du E, et al. Operation of a high renewable penetrated power system with CSP plants: a look-ahead stochastic unit commitment model. IEEE Trans Power Syst 2019;34(1):140–51.
[31] Li W, Wang Q. Stochastic production simulation for generating capacity reliability evaluation in power systems with high renewable penetration. Energy Convers Econ 2020;1(3):210–20.
[32] Quan H, Srinivasan D, Khosravi A. Incorporating wind power forecast uncertainties into stochastic unit commitment using neural network-based prediction intervals. IEEE Trans Neural Networks Learn Syst 2015;26(9):2123–35.
[33] Wang Q, Martinez-Anido CB, Wu H, Florita AR, Hodge B. Quantifying the economic and grid reliability impacts of improved wind power forecasting. IEEE Trans Sust Energy 2016;7(4):1525–37.
[34] Wang Q. Advances of wholesale and retail electricity market development in the context of distributed energy resources. Academic Press; 2021. p. 99–142.

[35] Costilla-Enriquez N, Ortega-Vazquez M, Tuohy A, Motley A, Webb R. Operating dynamic reserve dimensioning using probabilistic forecasts. IEEE Trans Power Syst 2022. https://doi.org/10.1109/TPWRS.2022.3163106.
[36] Power System Optimizer (PSO). [Online]. <https://psopt.com/>.
[37] Wang Q, Wu H, Florita A, Martinez-Anido C, Hodge B. The value of improved wind power forecasting: grid flexibility quantification, ramp capability analysis, and impacts of electricity market operation timescales. Appl Energy 2016;184:696–713.
[38] Philbrick CR. Wind integration and the need for advanced decision support tools. In: Proceedings of the 2011 IEEE power and energy society general meeting, Detroit, Michigan; 2011.
[39] Makarov YV, et al. Incorporating uncertainty of wind power generation forecast into power system operation, dispatch, and unit commitment procedures. IEEE Trans Sust Energy 2011;2(4):433–42.
[40] Yan X, Abbes D, François B. Uncertainty analysis for day ahead power reserve - quantification in an urban microgrid including PV generators. Renew Energy 2017;106:288–97.
[41] Matheson JE, Winkler RL. Scoring rules for continuous probability distributions. Manag Sci 1976;22(10):1087–96.
[42] Hobbs BF, et al. How can probabilistic solar power forecasts be used to lower costs and improve reliability in power spot markets? A review and application to flexiramp requirements. IEEE Open Access J Power Energy 2022;9:437–50.
[43] Hobbs BF, et al. Using probabilistic solar power forecasts to inform flexible ramp product procurement for the california ISO. Solar Energy Adv 2022;2:1–11.
[44] Li B, et al. Sizing ramping reserve using probabilistic solar forecasts: a data-driven method. Appl Energy 2022;313.